THE JOURNAL OF BIOLOGICAL CHEMISTRY VOL. 283, NO. 24, pp. 16682–16692, June 13, 2008
Printed in the U.S.A.

Decreased Ceramide Transport Protein (CERT) Function Alters Sphingomyelin Production following UVB Irradiation*

Received for publication, January 30, 2008, and in revised form, March 27, 2008 Published, JBC Papers in Press, April 14, 2008, DOI 10.1074/jbc.M800799200

Alexandra Charruyer[‡1], Sean M. Bell[‡1], Miyuki Kawano[§], Sounthala Douangpanya[‡], Ten-Yang Yen[¶], Bruce A. Macher[¶], Keigo Kumagai[§], Kentaro Hanada[§], Walter M. Holleran[‡‖], and Yoshikazu Uchida[‡2]

From the [‡]Department of Dermatology, School of Medicine, University of California, Northern California Institute for Research and Education, and Veterans Affairs Medical Center, San Francisco, California 94121, [‖]Department of Pharmaceutical Chemistry, School of Pharmacy, University of California, San Francisco, California 94143, [§]Department of Biochemistry and Cell Biology, National Institute of Infectious Diseases, Tokyo 162-8640, Japan, and [¶]Department of Chemistry and Biochemistry, San Francisco State University, San Francisco, California 94132

Increased cellular ceramide accounts in part for UVB irradiation-induced apoptosis in cultured human keratinocytes with concurrent increased glucosylceramide but not sphingomyelin generation in these cells. Given that conversion of ceramide to non-apoptotic metabolites such as sphingomyelin and glucosylceramide protects cells from ceramide-induced apoptosis, we hypothesized that failed up-regulation of sphingomyelin generation contributes to ceramide accumulation following UVB irradiation. Because both sphingomyelin synthase and glucosylceramide synthase activities were significantly decreased in UVB-irradiated keratinocytes, we investigated whether alteration(s) in the function of ceramide transport protein (or CERT) required for sphingomyelin synthesis occur(s) in UVB-irradiated cells. Fluorescently labeled *N*-(4,4-difluoro-5,7-dimethyl-4-bora-3*a*,4*a*-diaza-*s*-indacene-3-pentanoyl)-D-*erythro*-sphingosine (C_5-DMB-ceramide) relocation to the Golgi was diminished after irradiation, consistent with decreased CERT function, whereas the CERT inhibitor *N*-(3-hydroxy-1-hydroxymethyl-3-phenylpropyl)dodecanamide (1*R*,3*R* isomer) (HPA-12) produced an equivalent effect. UVB irradiation also induced the rapid formation of a stable CERT homotrimer complex in keratinocytes as determined by Western immunoblot and mass spectrometry analyses, a finding replicated in HeLa, HEK293T, and HaCaT cells and in murine epidermis. Ceramide binding activity was decreased in recombinant CERT proteins containing the UVB-induced homotrimer. The middle region domain of the CERT protein was required for the homotrimer formation, whereas neither the pleckstrin homology (Golgi-binding) nor the START (ceramide-binding) domains were involved. Finally like UVB-treated keratinocytes, HPA-12 blockade of CERT function increased keratinocyte apoptosis, decreased sphingomyelin synthesis, and led to accumulation of ceramide. Thus, UVB-induced CERT homotrimer formation accounts, at least in part, for apoptosis and failed up-regulation of sphingomyelin synthesis following UVB irradiation, revealing that inactive CERT can attenuate a key metabolic protective mechanism against ceramide-induced apoptosis in keratinocytes.

UV irradiation represents a major oxidative stressor for mammalian skin. The impact of UV irradiation has been demonstrated in conjunction with the pathogenesis of myriad cutaneous diseases, including photocarcinogenesis, photoaging, and photoallergy (1–3). Although UV irradiation-induced DNA damage may lead to the development of both melanoma and non-melanoma skin cancers (1, 2), UV irradiation also increases apoptosis via activation of death signaling pathways, *i.e.* NF-κB (4), Fas death receptor (5), or mitogen-activated protein kinase (MAPK) activation (6), initiated by alterations of plasma membrane functions (7). As such, UV-induced apoptosis can prevent carcinogenesis by eliminating potentially damaged or mutated cells (8). However, a recent study suggests that increased apoptosis in normal keratinocytes (KC)[3] can promote clonal expansion of mutated cells, resulting in increased tumorigenesis (9). Because both squamous and basal cell carcinoma cells are more resistant to apoptosis (10), the prevention of excess apoptosis in normal KC following oxidative stressors is important for decreasing the risk of tumorigenesis.

Ceramide (Cer) is the constituent backbone structure for all sphingolipids and is ubiquitously distributed in all mammalian cells/tissues. Alterations of cellular Cer levels in response to

* This work was supported, in whole or in part, by National Institutes of Health Grants AR 051077 (to Y. U.), PO1-AR39448 (to W. H.), and P20 MD000262 (to B. A. M.). This work was also supported by a Research Evaluation and Allocation Committee award from the University of California, San Francisco (to Y. U.) and National Science Foundation Grant CHEM-0619163 (to T.-Y. Y. and B. A. M.). The costs of publication of this article were defrayed in part by the payment of page charges. This article must therefore be hereby marked "*advertisement*" in accordance with 18 U.S.C. Section 1734 solely to indicate this fact.

[1] Both authors contributed equally to this work.

[2] To whom correspondence should be addressed: Dermatology Service and Research Unit (190), Veterans Affairs Medical Center, 4150 Clement St., San Francisco, CA 94121. Tel.: 415-750-2091; Fax: 415-751-3927; E-mail: uchiday@derm.ucsf.edu.

[3] The abbreviations used are: KC, keratinocytes; Cer, ceramide; CERT, ceramide transport protein; CHK, cultured human keratinocytes; GlcCer, glucosylceramide; SM, sphingomyelin; ER, endoplastic reticulum; START, steroidogenic acute regulatory protein (StAR)-related lipid transfer; PH, pleckstrin homology; MR, middle region; VAP, vesicle-associated membrane protein (VAMP)-associated protein; HPA-12, *N*-(3-hydroxy-1-hydroxymethyl-3-phenylpropyl)dodecanamide (1*R*,3*R* isomer); HPA-12 inactive, inactive 1*S*,3*R* isomer of HPA-12; C_5-DMB-Cer, *N*-(4,4-difluoro-5,7-dimethyl-4-bora-3*a*,4*a*-diaza-*s*-indacene-3-pentanoyl)-D-*erythro*-sphingosine; C_6-NBD-Cer, *N*-[12-[(7-nitro-2-1,3-benzoxadiazol-4-yl)amino]hexanoyl]-D-*erythro*-sphingosine; GFP, green fluorescent protein; WT, wild type; HA, hemagglutinin; PBS, phosphate-buffered saline; LC, liquid chromatography; ESI, electrospray ionization; MS/MS, tandem mass spectrometry; TLC, thin-layer chromatography.

specific stimuli, *e.g.* cytokine signaling, radiation, or oxidative stress, lead to cell cycle arrest, cellular differentiation, and apoptosis in a variety of cell types (11–13) including KC (14–16).

Given that cells, and in particular epidermal KC that reside at the interface with the external environment, are exposed to myriad risks and oxidative stressors, we hypothesized that these key skin cells deploy protective mechanisms against Cer-induced apoptosis. Metabolic pathways regulating the conversion of Cer to either sphingomyelin (SM) (17) or glucosylceramide (GlcCer) (18–20) and sphingosine to sphingosine 1-phosphate (21) can protect cells from Cer-induced apoptosis. These protective mechanisms exist not only in potentially carcinogenic cells but also in normal mammalian cells. We have shown that increasing the Cer-to-GlcCer conversion by bacterial sphingomyelinase overcomes Cer-induced inhibition of growth of human KC (22). In addition, we recently demonstrated that Cer hydrolysis, accompanied by conversion of sphingosine to sphingosine 1-phosphate, protects KC against UVB-mediated Cer-induced apoptosis.[4]

Because Cer is synthesized *de novo* at/in the endoplastic reticulum (ER) and is further converted to SM and GlcCer at the level of the Golgi, intracellular transport of Cer from ER to Golgi is a primary mechanism for the generation of both GlcCer and SM, involving both ATP-dependent and -independent mechanisms (23, 24). Recent studies reveal that the ATP-dependent Cer transport is mediated by the ceramide transport protein, CERT (25). CERT is a member of the family of steroidogenic acute regulatory protein (StAR)-related lipid transfer (START) proteins (26). The carboxyl-terminal region of CERT, consisting of 230 amino acids, contains the START domain and is responsible for stereospecific Cer binding (25, 27), whereas the amino-terminal region, consisting of 120 amino acids, contains the pleckstrin homology (PH) domain that binds phosphatidylinositol 4-monophosphate at the Golgi (25). The middle region (MR), between the PH and START domains, has a short peptide (FFAT) motif (25) that interacts with vesicle-associated membrane protein (VAMP)-associated protein (VAP) that is enriched in the ER (28). It has been suggested that sequences within the MR domain may promote the formation of coiled-coil structures (25). Moreover a recent study demonstrates that phosphorylation of serine and threonine residues within the MR domain down-regulates Cer transport (29). Thus, all three domains within CERT are required for Cer transport from the ER to Golgi.

We previously demonstrated that increased *de novo* Cer production accounts, in part, for the induction of apoptosis in cultured human keratinocytes (CHK) following UVB irradiation (16). However, *de novo* synthesized Cer also is converted to GlcCer and SM, both of which are major sphingolipid species and non-apoptotic Cer metabolites in keratinocytes. Importantly although GlcCer generation increases in CHK following UVB irradiation, SM generation is not changed (16). In the present study, we investigated 1) whether defects in the conversion of Cer to GlcCer and/or SM occur in CHK following UVB irradiation and thereby promote apoptosis and 2) the mechanism(s) responsible for the altered metabolic conversion(s). We demonstrate here that although both SM and GlcCer synthase activities were significantly decreased in CHK following UVB irradiation GlcCer generation increased in these cells. In addition, UVB irradiation decreased Cer transport from the ER to Golgi and induced the formation of a stable CERT homotrimer associated with decreases in Cer binding. Moreover a CERT trimer was generated not only in CHK but also in HeLa, HEK293T, and HaCaT cells as well as in murine epidermis following UVB irradiation. Furthermore the oxidative stressors H_2O_2 and NO also induced the formation of the stable CERT homotrimer complex in cells. Finally similar to UVB irradiation, blockade of CERT function increased apoptosis in CHK. These results reveal a novel mechanism that down-regulates SM synthesis in response to oxidative stress via alterations of CERT function through the formation of an inactive, stable homotrimer complex.

EXPERIMENTAL PROCEDURES

Materials—Cer and GlcCer were purchased from Sigma and Matreya (Pleasant Gap, PA), respectively. The CERT-specific inhibitor *N*-(3-hydroxy-1-hydroxymethyl-3-phenylpropyl)dodecanamide (1*R*,3*R* isomer) (HPA-12 inactive), CERT expression vectors, and anti-CERT antibody were generated as described previously (30). *N*-(4,4-Difluoro-5,7-dimethyl-4-bora-3*a*,4*a*-diaza-*s*-indacene-3-pentanoyl)-D-*erythro*-sphingosine (C_5-DMB-Cer), anti-Golgin 97, and Alexa 680-labeled goat anti-mouse antibodies were from Invitrogen. *N*-[12-[(7-Nitro-2-1,3-benzoxadiazol-4-yl)amino]hexanoyl]-D-*erythro*-sphingosine (C_6-NBD-Cer) was from Avanti Polar Lipids Inc. (Alabaster, AL) and Sigma. λ phage protein phosphatase was from New England Biolabs (Ipswich, MA). Sodium nitroprusside was from Sigma. High performance thin-layer chromatography (TLC) plates (Silica Gel 60) were from Merck.

Cell Culture and Transfection—Normal human keratinocytes were isolated from neonatal foreskins by a modification of the method of Pittelkow and Scott (31) under an Institutional Review Board-approved protocol (University of California, San Francisco). Cells were grown in keratinocyte growth medium supplemented with bovine epidermal growth factor, bovine pituitary extract, insulin, hydrocortisone, and 0.07 mM calcium chloride (Cascade Biologics, Portland, OR). The cultures were maintained at 37 °C under 5% CO_2 in air. Immortalized, non-transformed HaCaT cells derived from normal human keratinocytes (a gift from Dr. N. Fusenig, Heidelberg, Germany), HeLa cells, and human embryonic kidney cells (HEK293T) were cultured in Dulbecco's modified Eagle's medium supplemented with 10% fetal bovine serum. Cells were transfected with plasmids containing cDNA for GFP-fused (carboxyl-terminal) CERT wild type (WT), HA (amino-terminal)-tagged-CERT WT, FLAG (amino-terminal)-tagged CERT WT, FLAG-tagged CERT MR domain, or FLAG-tagged CERT ΔMR (lacking the MR domain), which were cloned into the expression vector pcDNA3.1(+) (25, 28) using FuGENE 6 transfection reagent (Roche Diagnostics).

Animals—Hairless mice (*Skh:hr-1*), 6–8 weeks old, were purchased from Charles River USA (Hollister, CA). Mice were

[4] E. Houben, P. M. Elias, W. M. Holleran, and Y. Uchida, submitted for publication.

fed Purina mouse diet (Ralston Purina Co., St. Louis, MO) and water *ad libitum*. Natural sunlight was excluded, and animals were exposed only to low levels of incandescent light prior to UVB irradiation. All animal experiments were performed under an Institutional Animal Care and Use Committee-approved protocol.

UVB Irradiation—UVB irradiation was performed as described previously (16, 32). Briefly cells were seeded ($2–4 \times 10^4$ cells/ml) in 4-well glass chamber slides or 100-mm culture dishes and maintained to 60–80% confluence. The cells were rinsed with phosphate-buffered saline (PBS) containing 0.07 mM calcium chloride followed by UVB irradiation (emission range, 280–340 nm; 305 nm maximum; FS 20/T12 bulbs, National Biological Co., Twinsburg, OH) in PBS with 0.07 mM calcium chloride. UVB exposure was measured using a Goldilux Ultraviolet radiometer (Oriel, Stratford, CT). Cells were exposed to a single UVB dose (60 mJ/cm^2) in most studies unless indicated otherwise. Immediately after UVB irradiation, PBS was replaced by culture medium. Purified His-tagged recombinant CERT protein (25) or murine epidermis was also irradiated with UVB as above. The dorsal skin of each mouse was irradiated with a single UVB dose equivalent to 150 mJ/cm^2 (32).

GlcCer Synthase and SM Synthase Assay—GlcCer synthase and SM synthase activities were determined as described previously (17). Briefly cell lysates prepared in a buffer containing 20 mM Tris/HCl (pH 7.5), 10 mM EGTA, 2 mM EDTA, and proteinase inhibitor mixture (Complete^{TM}, Roche Applied Science) were used as the enzyme source. GlcCer synthase and SM synthase activities were assayed using fluorogenic Cer (C_6-NBD-Cer) as the substrate. The reaction products were resolved in a solvent system that contained chloroform, methanol, and 12 mM $MgCl_2$ in H_2O (65:25:4, v/v/v). C_6-NBD-GlcCer and -SM were measured by using a Typhoon 9410 Multimodal Imager (Amersham Biosciences).

Immunofluorescence Microscopy—Cells transfected with CERT-GFP were fixed with 4% paraformaldehyde (w/v) in PBS for 10 min followed by permeabilization with 0.2% Triton X-100. Permeabilized cells were then incubated with mouse monoclonal anti-Golgin 97 at room temperature for 1 h and then with Alexa 680-labeled goat anti-mouse for 45 min. Control staining was performed with untransfected control cells for GFP and secondary antibody alone. Slides were examined with a Carl Zeiss LSM 510 confocal microscope (Carl Zeiss, Oberkochen, Germany). An argon laser at 488 nm and a helium-neon laser at 543 nm were used to excite GFP (emission, 515–540 nm) and Alexa 680 (emission, 680 nm), respectively.

Western Immunoblot Analysis—Western immunoblot analysis was performed using a procedure described previously (22). Briefly cells were lysed in lysis buffer (20 mM HEPES, 150 mM HCl, 10% glycerol, 1% Triton X-100, pH 7.8, and proteinase inhibitor mixture). 15–30 μg of total protein was resolved by electrophoresis on 10–12% SDS-polyacrylamide gels and electrophoretically transferred to polyvinylidene difluoride membranes (Invitrogen). Membranes were probed with either anti-CERT antibody, monoclonal anti-HA antibody (Cell Signaling Technology Inc., Danvers, MA), monoclonal anti-FLAG antibody, or monoclonal anti-β-actin antibody (Sigma), and proteins were detected using CDP-Star chemiluminescence (Invitrogen). Protein content was determined by BCA assay (Pierce).

Cer Transport—Cer transport was assessed using C_5-DMB-Cer as reported previously (25, 29, 33, 34) with modifications. Cells pretreated with or without 1 μM HPA-12 for 6 h were labeled with 1 μM C_5-DMB-Cer·bovine serum albumin complex (1:1) at 4 °C for 10 min and then washed with culture medium and PBS. Cells were irradiated with UVB at 4 °C in PBS followed by incubation with or without 1 μM HPA-12 at 37 °C for 30 min. Cells were fixed and examined by confocal microscopy as described above.

Cer Binding Assay—Binding of CERT to Cer was assessed by the method of Malakhova *et al.* (35) with modifications. C_5-DMB-Cer (1 mM) was dissolved in chloroform:methanol (9:1, v/v) in borosilicate glass tubes, dried under nitrogen to generate a Cer film immobilized on the glass, and further dried under vacuum for 1.5 h. Either UVB-treated or sham-treated purified recombinant CERT protein (50 μg) (25) in 0.5 ml of Tris/HCl buffer, pH 7.4, was added to the C_5-DMB-Cer film-coated tubes and incubated for various times at 37 °C. Fluorescence intensity generated in the aqueous protein fraction was measured spectrofluorometrically (excitation at 505 nm and emission at 511 nm).

Protein Identification by In-gel Digestion and Liquid Chromatography/Electrospray Ionization-Tandem Mass Spectrometry (LC/ESI-MS/MS) Analysis—Fractions containing immunoprecipitated CERT from UVB- or sham-irradiated cells were analyzed by SDS-PAGE as above. The resolved bands, stained with Coomassie Blue, were excised and digested with trypsin overnight at 37 °C. The resulting tryptic peptides were analyzed by LC/ESI-MS/MS using an LCQ or an LTQ ion trap mass spectrometer (Thermo Finnigan, San Jose, CA) with a nanoelectrospray ionization source. The LC analysis was conducted using a Micro-LC system (Micro-Tech Scientific, Sunnyvale, CA) or a Thermo Surveyor HPLC system. The resulting MS/MS spectra were searched against the National Center for Biotechnology Information (NCBI) non-redundant protein data base using the Sequest program to identify sequences of peptides.

Lipid Synthesis—To examine *de novo* sphingolipid synthesis following UVB irradiation, cells were cultured with [^{3}H]serine (1.5 μCi/ml), [9,10-^{3}H]palmitic acid (1.5 μCi/ml), or [^{3}H]galactose (1.5 μCi/ml) for the final 6 or 8 h. Lipids were extracted by the Bligh and Dyer method (36) with a modification described previously (16), and lipids were fractionated by high performance TLC as described previously (16). Radioisotope incorporated into each lipid fraction was measured by liquid scintillation spectroscopy. For *in vivo* studies, skin samples were obtained from euthanized animals at various time points before and 24 h after UVB exposure as described previously (37). Subcutaneous fat and fascia were removed by gentle scraping, and samples were floated dermis side down on keratinocyte growth medium containing 500 μM sodium acetate (34 μCi of sodium [^{14}C]acetate; Amersham Biosciences) for 2 h. Epidermis was separated from dermis following incubation in PBS (pH 7.4, 60 °C) for 30 s. Epidermal lipids were extracted, and the separation of individual lipid species was achieved by high perform-

TABLE 1

UVB irradiation decreases both GlcCer and SM synthase activities but increases GlcCer synthesis in CHK

CHK were treated with UVB. Details are described under "Experimental Procedures." Values represent mean ± S.D. from three experiments.

	SM synthase[a]	GlcCer synthase[a]	GlcCer synthesis[b]
	% of sham control	*% of sham control*	*% of sham control*
Sham	100.0 ± 10.5	100.0 ± 14.2	100.0 ± 10.5
UVB	77.6 ± 6.4[c]	37.2 ± 4.6[c]	162.3 ± 8.0[c]

[a] 8 h after irradiation, cells were harvested, and enzyme activities in cell homogenates were assayed.
[b] GlcCer synthesis was assessed by incorporation of [^{3}H]galactose (2 μCi/ml) into CHK for the final 3 h following irradiation.
[c] $p < 0.01$ *versus* sham-treated control.

ance TLC (37). Radioactivity was quantitated using a BAS Bioimage Analyzer (Fuji Film, Tokyo, Japan). Data are reported as photostimulated luminescence/cm^2 of epidermis.

Apoptosis Assay—Apoptosis was assessed by determining changes in cellular nuclear chromatin as described previously (38) using 2-(4-amidinophenyl)-1*H*-indole-6-carboxamidine and by terminal deoxynucleotidyltransferase-mediated digoxigenin-dNTP nick end labeling using the DNA Fragmentation Detection kit following the manufacturer's protocol (EMD Chemicals, Inc., Gibbstown, NJ). Approximately 100 cells chosen at random on each slide were counted per replicate, and the ratio of apoptotic to non-apoptotic cells was determined.

Statistical Analysis—Experiments were repeated at least three times. For each experiment, results from triplicate samples were expressed as the mean ± S.D. Significance between groups was determined with unpaired Student's *t* test.

RESULTS

SM but Not GlcCer Generation Decreased in Keratinocytes following UVB Irradiation—Our prior studies demonstrated that increased Cer production accounted for, in part, the induction of apoptosis in CHK following UVB irradiation (16). These studies also indicated that both the content and syntheses of Cer and GlcCer increased in CHK following UVB irradiation; however, SM generation remained unaltered (16). Given that the metabolic conversion of Cer to SM and/or GlcCer opposes Cer accumulation in keratinocytes, we hypothesized that restriction of Cer conversion to SM contributes to the Cer accumulation noted in CHK following UVB irradiation. Because SM synthesis/formation can be regulated by multiple steps, *e.g.* SM synthase activity or Cer transfer from the ER to the *trans*-Golgi and SM hydrolysis, we first studied SM synthase and GlcCer synthase activities in CHK 8 h following UVB irradiation when Cer and GlcCer levels both are known to be elevated (16). *In vitro* SM synthase activities were decreased by 22.4% compared with sham-irradiated control cells. Interestingly *in vitro* GlcCer synthase activity was also significantly decreased by 63.8% *versus* control (Table 1). To confirm our prior study showing an increase in GlcCer levels in UVB-treated CHK, GlcCer generation was assessed by [^{3}H]galactose incorporation in CHK following UVB irradiation. Again increased GlcCer generation was evident in these cells (Table 1). Thus, despite significant decreases in *in vitro* GlcCer synthase activity, increases in GlcCer generation in intact cells following UVB irradiation suggest that the available pool of Cer for GlcCer synthesis is greater than that for SM synthesis, possibly involving altered Cer transport within UVB-treated cells.

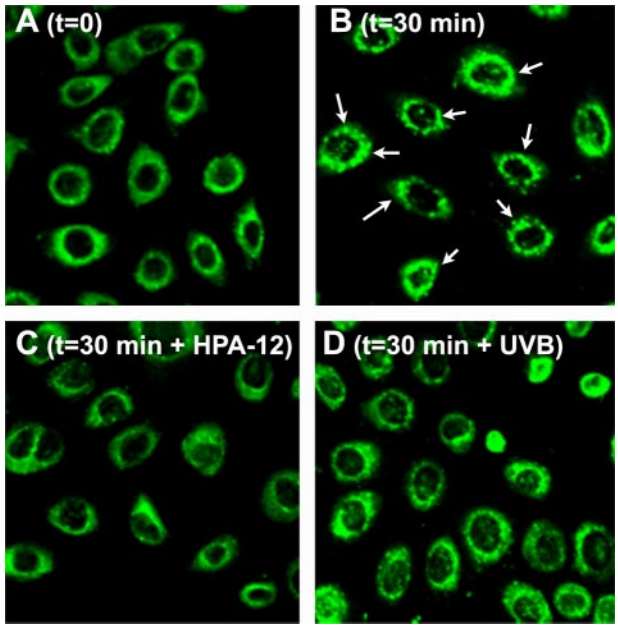

FIGURE 1. **Cer transport from the ER to the Golgi.** All cells (*A–D*) were incubated with C_5-DMB-Cer at 4 °C for 10 min to load with fluorescent Cer. Cells were sham-irradiated (*B* and *C*) or irradiated with 60 mJ/cm^2 (*D*) UVB followed by incubation at 37 °C for 30 min. Cellular localization of C_5-DMB-Cer was examined by confocal microscopy. *Arrows* indicate localization of C_5-DMB-Cer. *A*, cells were fixed and stained immediately after UVB irradiation. *B–D*, cells were fixed and stained 30 min after sham or UVB irradiation. CHK were pretreated with 10 μM HPA-12 (*C*), an inhibitor of CERT (30), for 6 h. Similar to prior studies demonstrating that C_5-DMB-Cer concentrates in the Golgi apparatus (25, 33, 34, 39), C_5-DMB-Cer appears in a punctate, perinuclear pattern in control cells incubated at 37 °C for 30 min (*B*). In addition, as shown in Fig. 2, CERT is also distributed perinuclearly, and this distribution is not altered in cells following UVB irradiation. However, C_5-DMB-Cer was not concentrated at perinuclear regions in UVB-irradiated CHK (*D*) as well as in cells treated with CERT inhibitor (*C*). Additional details are available under "Experimental Procedures."

UVB Irradiation Diminished Cer Transfer from the ER to the Golgi—Because the Cer transport pathways from the ER to the Golgi to synthesize SM and GlcCer are distinctly CERT-dependent and -independent, respectively (25), we next determined whether altered Cer transport from ER to *trans*-Golgi by a CERT-dependent pathway could account for the decreased SM generation in CHK following UVB treatment. As shown previously (25, 33, 34, 39), C_5-DMB-Cer was localized to the cytoplasm and the ER in CHK 10 min after incubation at 4 °C (Fig. 1*A*) and was subsequently redistributed to perinuclear regions, *i.e.* Golgi, 30 min following the increase in ambient temperature from 4 to 37 °C (Fig. 1*B*). In contrast, blockade of CERT function using a specific inhibitor of CERT, HPA-12 (Fig. 1*C*), showed decreased distribution of fluorescence to Golgi compared with sham-irradiated control cells (Fig. 1*B*). Moreover the Golgi-localized fluorescence was less intense in CHK irradiated with UVB (Fig. 1*D*) compared with that in sham-irradiated control cells (Fig. 1*B*), whereas decreases in fluorescent signals at perinuclear regions were not significant in UVB-irradiated cells compared with HPA-12-treated cells. We ascertained that UVB irradiation alone did not alter the fluorescence intensity of C_5-DMB-Cer because total cellular fluores-

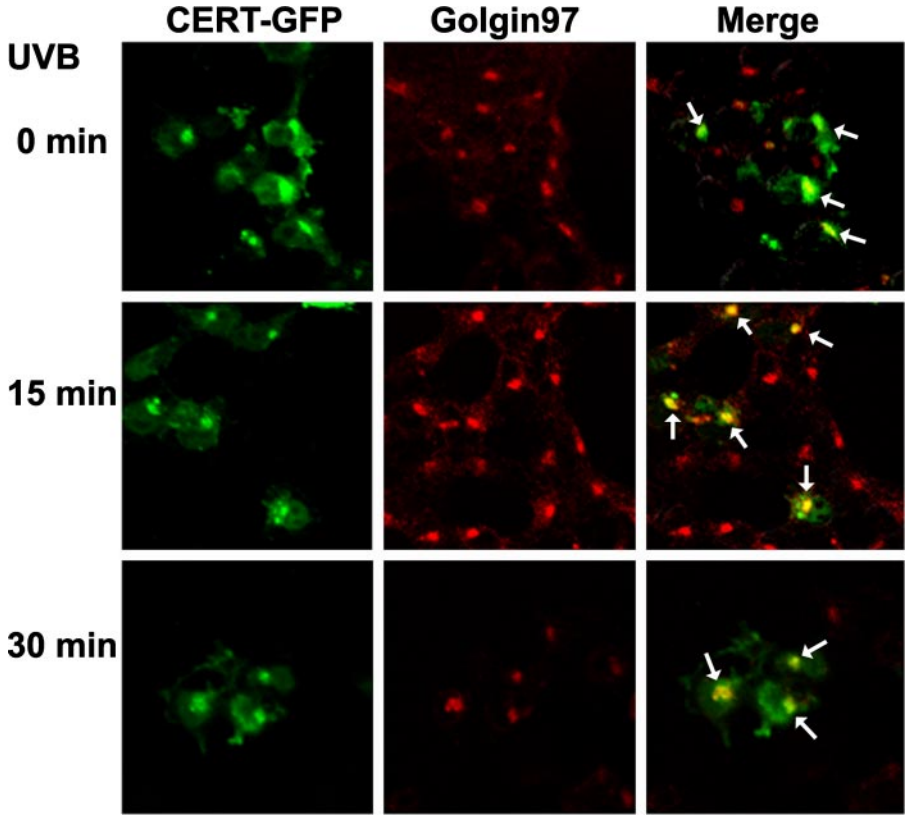

FIGURE 2. **CERT localization at the Golgi apparatus.** HEK293T cells were transfected with a GFP-CERT expression plasmid and treated with UVB as in Fig. 1. *Arrows* indicate colocalization of GFP-CERT and Golgi marker Golgin 97. Cells were fixed and stained with Golgin 97 and Alexa 680-labeled secondary antibody 15 or 30 min following irradiation. Additional details are available under "Experimental Procedures."

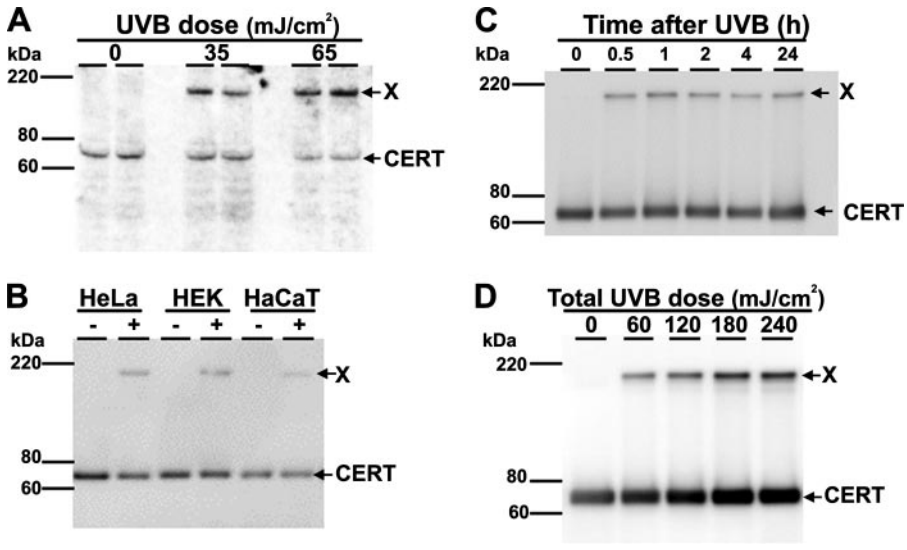

FIGURE 3. **Stable, high molecular weight CERT complex in UVB-treated cells.** Cells (cultured primary human keratinocytes (*A*); HeLa, HEK293T, and HaCaT cells (*B*); and HEK293T cells (*C*)) were treated with UVB as in Fig. 1. HeLa cells were treated multiple times with a UVB dose (60 mJ/cm2) with a 0.5-h time interval between treatments (*i.e.* one, two, three, or four repeat UVB exposures giving the indicated final UVB doses) (*D*). HeLa, HEK293T, and HaCaT cells were transfected previously with HA-tagged CERT. Cell lysates were prepared at 7 h (*A*), 1 h (*B*), or the indicated time points (*C*) following irradiation or 0.5 h after the last irradiation. SDS-PAGE was performed under reducing and denaturing conditions, and membranes were probed with anti-CERT (*A*) or anti-HA (*B–D*) antibodies followed by alkaline phosphatase-labeled secondary antibodies detected using CDP-Star chemiluminescence. Additional details are available under "Experimental Procedures."

cence did not change (data not shown). These results suggest that UVB irradiation diminishes CERT-dependent Cer transport from ER to Golgi in CHK.

UVB Irradiation Does Not Interfere with CERT Localization at the Golgi—We next investigated whether decreased Cer transfer to the Golgi is due to a modification of cellular CERT localization following UVB irradiation. HEK293T cells transiently transfected with a CERT-GFP expression plasmid were irradiated with UVB. CERT-GFP protein was localized at the Golgi (as determined by anti-Golgin 97 antibody colocalization) in cells at both 15 and 30 min following treatment (Fig. 2). Thus, cellular CERT-GFP localization appears to be normal following UVB irradiation.

UVB Irradiation Induced the Formation of a Stable CERT Homotrimer—To investigate whether UVB irradiation alters CERT protein levels in CHK, Western immunoblot analyses were performed under denaturing conditions. CERT levels were not significantly changed in CHK 7 h following a lower dose irradiation (35 mJ/cm^2) but modestly decreased in cells treated with a higher UVB dose (65 mJ/cm^2) compared with sham-irradiated control cells (Fig. 3*A*). However, in addition to a band corresponding to native CERT (≈68 kDa), an unknown band ("X") with an estimated molecular size of ≈200–210 kDa (Fig. 3*A*) was observed after irradiation at both lower and higher UVB doses. Band X was produced after UVB irradiation not only in CHK but also in other cells such as HA-tagged CERT WT-transfected spontaneously immortalized (HaCaT) human keratinocytes, HeLa cells, and HEK293T cells (Fig. 3*B*). A time course study revealed that band X was evident as early as 30 min following irradiation and that significant levels remained at least 24 h after irradiation (Fig. 3*C*).

Because it is likely that band X formation is increased in cells treated with a higher UVB dose (Fig. 3*A*), we investigated the dose dependence for generation of this unknown band in HeLa cells. Because increases in a single dose of UV irradiation over 100 mJ/cm^2 can cause acute deleterious effects in cells, including cell detachment and/or cell lysis, cells were instead treated mul-

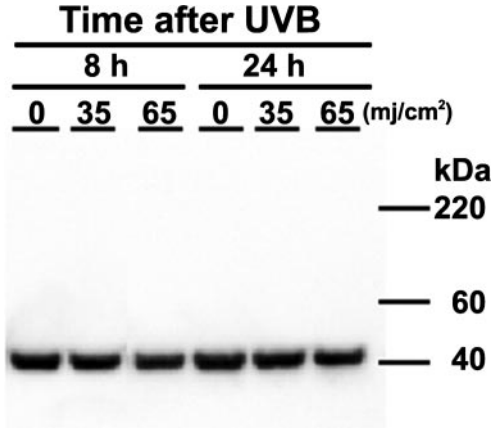

FIGURE 4. **β-Actin does not form stable, high molecular weight complexes in UVB-treated cells.** Cell lysates were prepared from UVB-treated CHK, and Western immunoblot analysis was performed using anti-β-actin monoclonal antibody. Only a single β-actin monomer (42-kDa) band was evident. Details are presented under "Experimental Procedures."

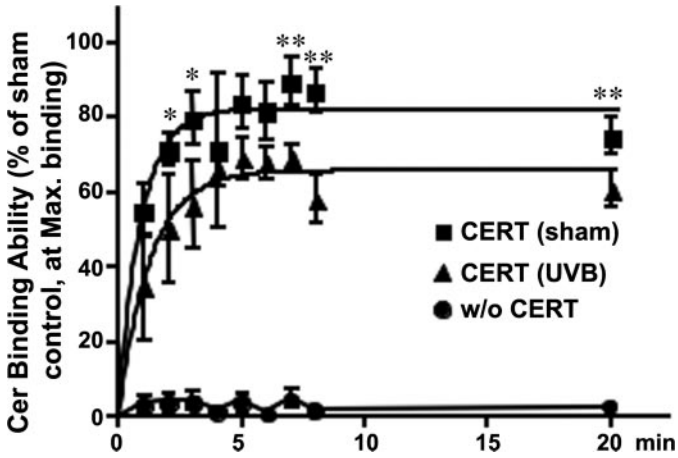

FIGURE 5. **Cer binding activity decreases in CERT following UVB irradiation.** Recombinant His-tagged CERT protein was suspended in PBS and treated with UVB. Results are representative of three independent experiments and reported as percentage of sham-irradiated control (maximum set to 100%). Values are mean ± S.D. ($n = 3$). *, $p < 0.05$; **, $p < 0.01$ *versus* corresponding UVB-treated CERT. Details are presented under "Experimental Procedures."

tiple times with a lesser UVB dose of 60 mJ/cm^2 with a 0.5-h time interval between treatments (*i.e.* one, two, three, or four times). Increases in CERT complex formation were evident with up to three repeat UVB exposures (Fig. 3*D*).

We next investigated whether band X was comprised of CERT alone, CERT and other protein(s), or nonspecific protein aggregates. Following UVB irradiation, FLAG-CERT was immunoprecipitated from HEK293T cells transfected with FLAG-tagged CERT WT and subsequently resolved by SDS-PAGE. The most intense band with a molecular mass of ≈69 kDa present in both UV-treated and sham-irradiated control cells was identified as CERT by in-gel tryptic digestion and LC/ESI-MS/MS analysis (data not shown). Twenty-nine tryptic peptides, spanning between amino acids 49 and 626, were detected that reflected sequence coverage of 60.7%, demonstrating a high degree of data confidence. In addition to the expected ≈69-kDa band, a less intense band with a high molecular mass, ≈200–210 kDa, corresponding to band X (see Fig. 3*A*) was found only in the UVB-treated samples. This band was also identified as CERT. Eight tryptic peptides, spanning between amino acids 49 and 595, were detected with sequence coverage of 25.3%. Peptides from other proteins were not found in this band revealing band X to be a stably cross-linked CERT homocomplex. Estimation of molecular size by SDS-PAGE and size exclusion chromatography (data not shown) suggests that homotrimer formation occurs in CERT following UVB irradiation. These results demonstrate that UVB irradiation induces the formation of a stable cross-linked CERT homotrimer rather than causing a significant decrease in cellular CERT protein levels. Moreover in contrast to CERT protein, only a single band is evident for β-actin with no evidence of higher molecular weight complex formation following UVB irradiation (Fig. 4).

Cer Binding Activity Decreases in CERT following UVB Irradiation—To investigate whether the formation of the stable CERT homotrimer accounts for decreased SM generation in CHK following UVB irradiation, we compared the Cer binding ability of UVB- (+) and sham-irradiated (−) CERT proteins. Purified recombinant CERT protein was treated with UVB *in vitro*. LC-MS/MS analysis demonstrated that a band at ~210 kDa was formed following UVB irradiation consisting solely of the CERT protein (data not shown) as noted above. Approximately ≈20% of the CERT protein was converted to the CERT homotrimer form as determined by Western immunoblot analysis. Consistent with the formation of the stable CERT homotrimer at ≈20% of total CERT following UVB treatment, Cer binding activity of irradiated CERT (containing both the stable CERT homotrimer and intact CERT in a ratio of ~2:8 as above) decreased to ≈80% of sham-irradiated CERT control ($p < 0.01$) (Fig. 5). Thus, it is likely that the ability of CERT to bind Cer is significantly deceased in the stable homotrimeric protein complex.

MR of CERT Protein Is Required for Homotrimer Formation—CERT protein consists of PH, MR, and START domains (Fig. 6*A*), which are responsible for binding to/association with the Golgi, ER, and Cer, respectively (25, 27). To investigate which domain(s) is(are) required for CERT homotrimer formation, we used both HEK293T and HeLa cells transfected with either FLAG-tagged CERT WT; FLAG-tagged CERT ΔMR, which lacks the MR domain; or FLAG-tagged CERT MR that expresses only the MR domain. UVB irradiation induced the formation of large CERT multimer complexes in both HEK293T and HeLa cells transfected with either FLAG-tagged CERT WT (Fig. 6*B*, *lanes 4* and *6*) or FLAG-tagged CERT MR (molecular size for the resultant peptide is ~30 kDa in monomer form) (Fig. 6*B*, *lanes 12* and *14*), whereas CERT trimer or multimers were not detected in cells transfected with FLAG-tagged CERT ΔMR (Fig. 6*B*, *lanes 8* and *10*). These results reveal that the MR of the CERT protein contains an epitope/sequences responsible for the UVB-induced stable homotrimer formation, whereas the PH and START domains are not required for this stable association.

UVB Irradiation Does Not Affect CERT Phosphorylation/Dephosphorylation—Because a recent study demonstrated that the transport activity of Cer from the ER to the *trans*-Golgi by CERT is regulated by phosphorylation, *i.e.* down-regulated by

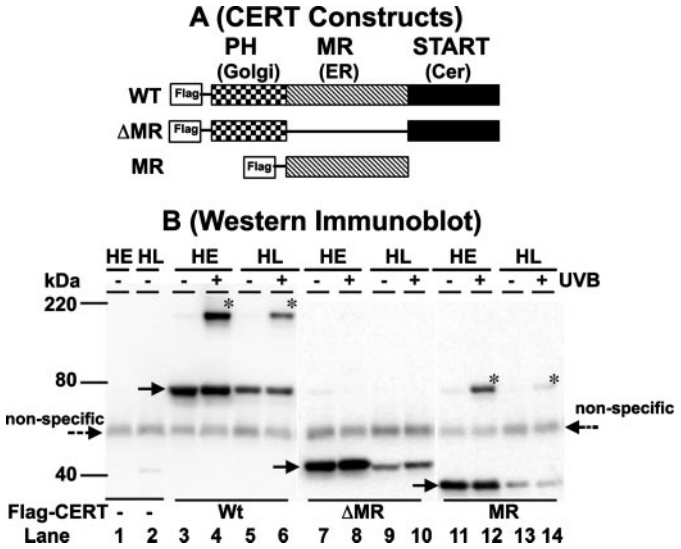

FIGURE 6. **Homotrimer formation occurs within the middle region of CERT.** *A*, CERT-FLAG constructs. WT construct expresses all three CERT domains, *i.e.* the PH domain that binds phosphatidylinositol 4-monophosphate at the *trans*-Golgi, the MR domain that contains an FFAT motif for binding to VAP enriched in the ER, and the Cer-binding START, whereas MR construct expresses only the MR domain; each construct also contains a FLAG sequence tag. The ΔMR construct contains the PH and START domains linked to the FLAG tag but lacks the MR domain. *B*, stable CERT trimer formation was evident in both WT- and MR- but not ΔMR-expressing cells following UVB irradiation. HEK293T (*HE*) or HeLa cells (*HL*) cells were transfected with FLAG-tagged CERT WT, FLAG-tagged CERT ΔMR, or FLAG-tagged CERT MR plasmids followed by irradiation with UVB as above. CERT protein was immunoprecipitated with anti-FLAG antibody and analyzed by Western immunoblot with anti-FLAG antibody. *Arrows* and *asterisks* indicate CERT monomer and the stable CERT homotrimer, respectively. *Lanes 3–6*, FLAG-WT monomer (*arrow*) and multimer (*asterisks*) after UVB irradiation; *lanes 7–10*, FLAG ΔMR monomer only (*arrow*) with no multimer formed following UVB irradiation in either the HEK293T or HeLa cell line; *lanes 11–14*, MR monomer (*arrow*) and multimer (*asterisks*) formed when only FLAG-MR domain is expressed. A nonspecific band was observed in all samples (*dotted arrows*) including non-transfected cells (*left lanes*). Details are presented under "Experimental Procedures."

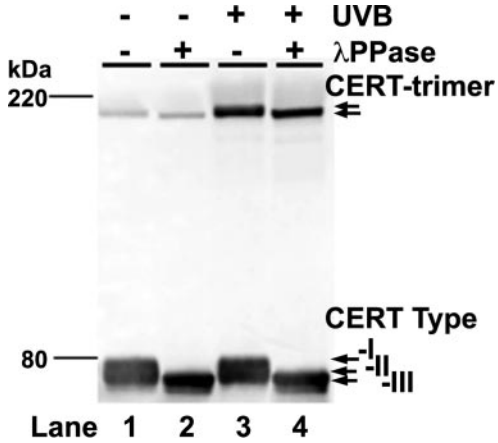

FIGURE 7. **UVB irradiation does not affect CERT phosphorylation.** Both type I and II forms of CERT are present at approximately equal levels in HEK293T following sham or UVB irradiation (*lanes 1* and *3*, respectively), whereas the dephosphorylated form (type III) of CERT is evident in these cells only after λ phage protein phosphatase (λ*PPase*) treatment. HEK293T cells transfected with FLAG-tagged CERT WT were irradiated with UVB as above. Cell lysates were then treated with (*lanes 2* and *4*) or without (*lanes 1* and *3*) λ phage protein phosphatase (800 units) at 30 °C for 30 min (29). FLAG-tagged CERT was detected by Western immunoblotting analysis using anti-FLAG antibody. Additional details are presented under "Experimental Procedures."

phosphorylation and up-regulated by dephosphorylation (29), we next investigated whether UVB irradiation alters the phosphorylation status of CERT. Consistent with the prior study, two CERT bands, corresponding type I CERT (highly phosphorylated form) and type II CERT (less phosphorylated form) (29), were detected at an approximately equivalent ratio (type I:type II = 0.44:0.56) in sham-irradiated HEK293T cells transfected with FLAG-tagged CERT WT (Fig. 7, *lane 1*). These CERT proteins are converted to type III CERT (dephosphorylated form) (29) following λ phage protein phosphatase treatment (Fig. 7, *lane 2*). Similar to the results in sham-irradiated control cells, type I and II bands were again present at an approximately equal ratio (type I:type II = 0.50:0.50) in UVB-treated cells (Fig. 7, *lane 3*), and these proteins were converted to type III by λ phage protein phosphatase treatment (Fig. 7, *lane 4*). Moreover the CERT homotrimer band was also shifted to a lower molecular size following λ phage protein phosphatase treatment (Fig. 7, *lanes 1* and *3 versus lanes 2* and *4*, respectively). Thus, it is unlikely that alterations of phosphorylation/dephosphorylation affect CERT-mediated Cer cellular trafficking and/or CERT multimer formation following UVB irradiation.

Blockade of CERT Function Induced Apoptosis—We next investigated whether the CERT-dependent conversion of Cer to SM can regulate cellular Cer levels and thereby protect cells against Cer-induced apoptosis in CHK. As anticipated, the inhibition of CERT function using HPA-12 specifically decreased SM synthesis in parallel with increased Cer levels in CHK, whereas GlcCer synthesis was not altered 8 h after treatment (Table 2). In contrast, the inactive stereoisomer of HPA-12 did not affect the synthesis of these lipids (Table 2). Consistent with our prior studies, increased apoptosis was evident in UVB-irradiated cells (Fig. 8 and Ref. 16); in addition, increased apoptosis was also evident in CHK incubated with 10 μM HPA-12 (Fig. 8), but the inactive stereoisomer showed no effect, suggesting that the inhibition of CERT function leads to both decreased SM generation and increased Cer levels, which in turn are coincident with increased apoptosis. These results reveal an ongoing role for CERT-mediated transfer of Cer for SM synthesis and a role for CERT in regulating Cer-mediated apoptosis.

Oxidative Stress Induced CERT Trimer Formation—Prior studies demonstrated that other oxidative stressors, *i.e.* NO (40) and H_2O_2 (41) as well as UVB irradiation (16), increase Cer-mediated apoptosis. We therefore investigated whether other general oxidative stressors, specifically NO and H_2O_2, also induce the formation of the stable CERT homotrimer in cells. Similar to the results of UVB treatment noted above, stable CERT homotrimer was evident in HEK293T cells exposed to either H_2O_2 (Fig. 9, *lane 2*) or the NO generator sodium nitroprusside (Fig. 9, *lane 3*). Thus, oxidative stress induced by UVB irradiation or chemical treatment can promote the formation of the inactive stable CERT homotrimer.

CERT Homotrimer Formation and Decreased SM Generation Occur in Murine Epidermis following UVB Irradiation—Finally we investigated whether the stable CERT homotrimer is formed in intact epidermis following UVB irradiation. Similar to the results in cultured human keratinocytes, a stable CERT homotrimer was evident in epidermis isolated

TABLE 2

Inhibition of CERT by HPA-12 specifically blocks SM synthesis

CHK were treated with 2.5 μM HPA-12 active, HPA-12 inactive, or vehicle for 8 h. Cells were cultured with [^{3}H]palmitic acid (1.5 μCi/ml) for the final 4 h of treatment. Values represent mean ± S.D. from three experiments.

	Incorporation of [^{3}H]palmitate into sphingolipids		
	SM	Cer	GlcCer
	cpm × 10^5*/plate* (*% of vehicle control*)		
Sham	21.45 ± 1.17 (100 ± 5.4)	5.42 ± 0.73 (100 ± 13.5)	5.63 ± 0.48 (100 ± 8.4)
HPA-12 active	3.72 ± 0.22[a] (17.3 ± 2.1)[a]	6.76 ± 0.27[a] (124.8 ± 5.0)[a]	5.50 ± 0.17 (97.8 ± 3.0)
HPA-12 inactive	21.43 ± 1.33 (99.9 ± 6.2)	5.68 ± 0.16 (104.9 ± 3.0)	6.10 ± 0.16 (108.4 ± 2.8)

[a] $p < 0.01$ *versus* vehicle-treated control.

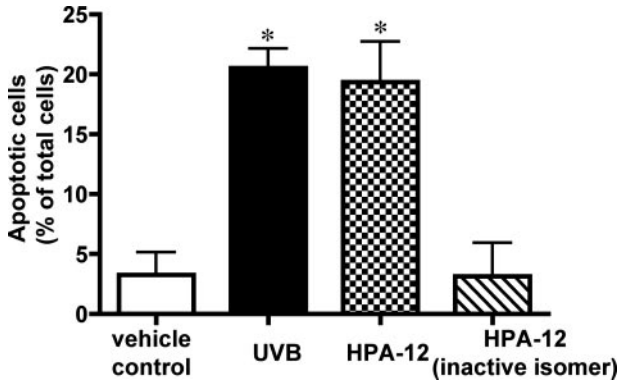

FIGURE 8. **Blockade of CERT function induces apoptosis.** CHK were treated with vehicle, 10 μM HPA-12 active, 10 μM HPA-12 inactive, or UVB as above. Apoptotic cells were assessed by terminal deoxynucleotidyltransferase-mediated digoxigenin-dNTP nick end labeling 6 h following treatment. Apoptotic cells are reported as the percentage of the total number of 2-(4-amidinophenyl)-1*H*-indole-6-carboxamidine-positive cells; results are representative of three independent experiments (mean ± S.D., $n = 3$). *, $p < 0.01$ *versus* corresponding vehicle controls. Details are presented under "Experimental Procedures."

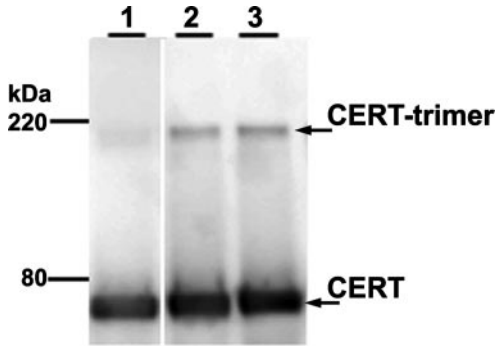

FIGURE 9. **Both H_2O_2 and NO also generate CERT trimer formation.** HEK293T cells were transfected with FLAG-tagged CERT WT plasmid and treated with vehicle (*lane 1*), 750 μM H_2O_2 (*lane 2*), or 0.5 μM sodium nitroprusside, an NO generator (*lane 3*). CERT protein was analyzed 3 h following treatment by Western immunoblot analysis. Details are presented under "Experimental Procedures."

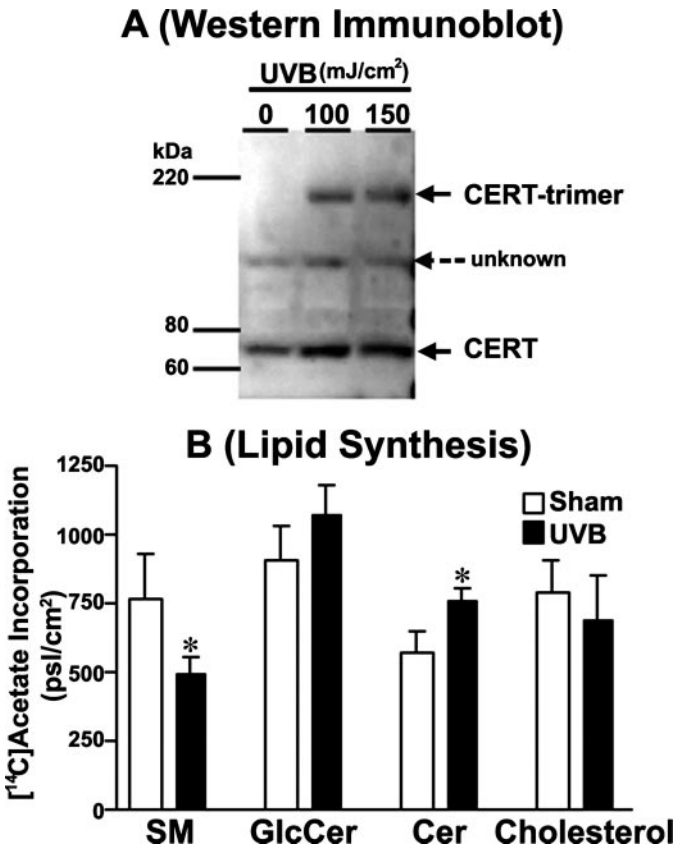

FIGURE 10. *A*, Western immunoblot analysis. Dorsal mouse skin was excised from euthanized animals, placed on a culture dish, and irradiated with UVB (0, 100, or 150 mJ/cm^2) as described above for CHK. Epidermal homogenates were then prepared from skin 1 h following treatment. SDS-PAGE was performed under denaturing conditions, and a membrane was probed with anti-CERT and alkaline phosphatase-labeled secondary antibody as above. CERT monomer and CERT trimer bands are indicated by *lower* and *upper arrows*, respectively; an unknown alkaline phosphatase positive band is also noted (*dotted line arrow*). *B*, lipid synthesis. Dorsal mouse skin was irradiated with UVB (150 mJ/cm^2) as above. To assess rates of lipid synthesis, skin samples were taken before and 24 h after UVB exposure and then incubated with keratinocyte growth medium containing sodium [^{14}C]acetate for 2 h. Epidermal lipids were extracted, and the separation of individual lipid species was achieved by high performance TLC. Data are reported as photostimulated luminescence (*psl*)/cm^2 of epidermis (mean ± S.D., $n = 5$). *, $p < 0.01$ *versus* non-irradiated controls. Additional details are available under "Experimental Procedures."

from murine skin irradiated with UVB *ex vivo* (Fig. 10*A*). To investigate whether UVB irradiation also leads to similar alterations in CERT function *in vivo* as noted in CHK (above), we assessed the synthesis of SM in whole epidermis. Because our prior studies showed that epidermal DNA synthesis decreases during the first 0.5–12 h, returns to normal levels at 24 h, and then increases at 36–48 h following irradiation (32), we determined lipid synthesis at 22–24 h when DNA synthesis is not significantly altered to avoid cellular proliferation-mediated changes in lipid synthesis. Similar to the results observed in UVB-irradiated CHK, SM but not GlcCer synthesis was significantly decreased, whereas Cer generation was increased in epidermis following UVB treatment to intact murine skin (Fig. 10*B*). In comparison, cholesterol synthesis was not significantly altered by UVB irradiation (Fig. 10*B*). These results indicate that the formation/presence of the CERT homotrimer is associated with suppression of SM synthesis and increased Cer production

both in epidermis *in vivo* and in cultured human keratinocytes (shown above).

DISCUSSION

The metabolic conversion of Cer to either SM or GlcCer is not only required for the generation of cellular membranes constituents but also is important for the homeostatic regulation of cellular Cer levels, thereby reducing the risk of Cer-induced apoptosis (17–20). Our prior studies showed not only increased Cer production in CHK but also significantly elevated GlcCer generation in UV-irradiated cells (16). SM levels, however, were not elevated following UVB irradiation (16), suggesting that the SM and GlcCer synthetic pathways are independently regulated. We report here a mechanism(s) that accounts for the apparent failure to up-regulate SM production following UVB irradiation that appears linked to the subsequent UVB-induced apoptosis. Because the major pathways that transfer Cer from ER to Golgi for either SM or GlcCer synthesis appear to be distinct, *i.e.* CERT is required for the majority of Cer transfer from the ER to the *trans*-Golgi for SM synthesis, whereas CERT-independent transport accounts for the bulk of Cer transport for GlcCer synthesis (23, 24), we have focused on alterations of CERT function induced by UVB irradiation. We demonstrate that UVB irradiation induced the formation of a stable CERT homotrimer complex associated with decreases in both cellular transfer of Cer from ER to Golgi and Cer binding ability. We also show that blockade of CERT function using a specific CERT inhibitor mimicked UVB-induced apoptosis in CHK. Moreover similar to the results in cultured keratinocytes, *in vivo* studies also revealed the presence of a stable CERT homotrimer in association with increased Cer formation/content and decreased SM (but not GlcCer) generation in UVB-irradiated murine epidermis. Together with our prior studies, these findings strongly suggest that a modification of CERT function by the formation of a stable homotrimer complex contributes to the decrease in SM synthesis and accumulation of Cer, resulting in increased apoptosis following UVB irradiation. In addition, because H_2O_2 and NO also induced the formation of an equivalent CERT homotrimer, the formation of this (inactive) trimer complex represents a potential risk factor in the apoptosis that occurs subsequent to oxidative stress exposure.

In addition to CERT function, SM synthase or GlcCer synthase activities also represent rate-limiting factors for metabolic conversion of Cer to either SM or GlcCer, respectively. Interestingly both SM synthase and GlcCer synthase activities decreased in UVB-irradiated CHK (Table 1). However, despite the large decrease in GlcCer synthase *in vitro* enzyme activity, GlcCer generation was significantly increased following UVB irradiation, suggesting that diminished Cer transport in the SM synthesis pathway could provide an increased pool of available Cer for GlcCer production. Our prior studies demonstrated that sphingolipid synthesis (including GlcCer) is up-regulated following acute epidermal permeability barrier perturbation to restore barrier function, whereas serine palmitoyltransferase but not GlcCer synthase activity is increased (42). These results suggest that basal GlcCer activity is sufficient to up-regulate GlcCer production in epidermal keratinocytes without measurable changes in total enzyme activity *in vitro*. Thus, it is likely that despite a measured decrease in GlcCer synthase activity residual enzyme activity can suffice to generate GlcCer in response to any increases in the available Cer pool in keratinocytes following UV irradiation. It has been suggested that a CERT-independent pathway may also supply Cer for SM synthesis in cells (43). However, inhibition of CERT significantly inhibited SM generation while leaving GlcCer production unaltered in keratinocytes (Table 2), suggesting that HPA-12-sensitive Cer transport, *i.e.* CERT-dependent transport, is important for SM synthesis in keratinocytes. Hence although the relative contribution of either decreased SM synthase activity or altered CERT function to the diminished SM generation following UVB irradiation has not been determined, the stable CERT homotrimer formation represents a previously unrecognized negative regulatory mechanism in SM synthesis homeostasis.

Although prior studies have shown that the START domain of CERT binds Cer (25), our present study revealed that the MR domain is required for the stable CERT homotrimer formation that accompanies decreased Cer binding activities. Thus, it appears that conformational changes in the CERT molecule induced by oxidative stress rather than direct effects on the Cer binding domain itself can affect Cer binding. However, the current results do not exclude the possibility that altered interaction between either the PH domain and phosphatidylinositol 4-monophosphate at the *trans*-Golgi (25) or the FFAT motif in the MR domain and VAP at the ER (28) can affect CERT trafficking between the ER and the *trans*-Golgi, which could also result in decreased SM generation. Although CERT function also could be modulated by alteration of cellular phosphatidylinositol 4-monophosphate profiles, our results demonstrate that CERT still localizes to the Golgi, whereas abnormal localization of CERT to the nucleus, mitochondria, and/or plasma membrane was not evident following UVB irradiation. Thus, UVB irradiation does not appear to significantly alter the intracellular trafficking of CERT. It appears more likely that decreased overall Cer binding activity, due to the stable homotrimer formation, is the mechanism primarily responsible for decreasing Cer transfer from the ER to the *trans*-Golgi for SM generation following UVB irradiation and possibly other oxidative stressors.

We have demonstrated here that the CERT homotrimer is stable under both denaturing and reducing conditions as used in electrophoresis. Such results strongly suggest that the CERT complex formation is due to intermolecular covalent bonds, perhaps through dityrosine and/or ditryptophan linkages, rather than hydrogen bonding and/or thioester linkages. Although it is possible that CERT forms stable complexes with other proteins including VAP enriched at the ER, LC-MS/MS analysis revealed that the high molecular weight CERT complex consists solely of CERT proteins. Although the association of the CERT complex with other protein(s) cannot be excluded, the present studies suggest that a molecular interaction between individual CERT molecules occurs more frequently or at higher affinity compared with any interaction(s) between CERT and other protein(s). Because sequence analysis revealed that the region in the MR domain between amino acids 271 and 302 shows a high probability for forming coiled-coil structures

(44) (data not shown), a portion of CERT monomer may already exist as homotrimers, albeit as non-stable/reversible complexes, at basal conditions. Moreover because UVB irradiation, H_2O_2, and NO all induce the formation of a stable trimer complex, reactive oxygen species produced by oxidative stress may promote the stable intermolecular bonding of CERT. However, the details regarding the particular moieties involved remain to be determined. Moreover it should be noted that a larger complex(es) of a key structural protein, β-actin, were not generated in cells following UVB irradiation. Thus, a stable cross-linked complex(es) is only formed for specific protein species.

Recent findings reveal that CERT function also is regulated by phosphorylation with dephosphorylation resulting in the activation of CERT function (29, 45). Interestingly perturbation of SM/cholesterol rafts induced CERT dephosphorylation, resulting in increasing SM generation (29). Whereas UV irradiation has been shown to decrease SM in raft microdomains to generate Cer (14), we have shown here that no significant changes in CERT phosphorylation status occurred after irradiation, suggesting that the SM/cholesterol raft-mediated CERT activation pathway is not significantly affected in cells following UVB irradiation. More importantly because UVB irradiation did not increase CERT phosphorylation, the decreases in SM generation cannot be ascribed to inactivation of CERT function via phosphorylation in UVB-irradiated cells. Coincidentally similar to CERT monomer(s), the CERT trimer was dephosphorylated by exogenous phosphatase treatment. Hence although *in vitro* phosphatase activity may not exactly mimic that *in vivo*, it is unlikely that increased resistance of the CERT homotrimer complex to phosphatase *in vivo* could represent the primary mechanism for the observed decrease in CERT function following oxidative stress.

Despite significant decreases in SM synthesis (83%) in the cells by CERT inhibition using HPA-12, Cer increased by 25%, whereas GlcCer production did not change (Table 2), suggesting that suppression of the Cer-to-SM metabolic pathway could stimulate other Cer metabolic pathways, *e.g.* Cer hydrolysis, followed by sphingosine-to-sphingosine 1-phosphate generation. We previously reported that epidermal keratinocytes express all isoforms of ceramidase that have so far been characterized in mammalian species (46), suggesting that Cer can be hydrolyzed at/in ER/Golgi by alkaline ceramidase, in mitochondria and/or at the plasma membrane by neutral ceramidase, and in lysosomes by acidic ceramidase. We also recently demonstrated increases in Cer hydrolysis to sphingosine (followed by its conversion to sphingosine 1-phosphate) in keratinocytes in response to UV irradiation.[4] Thus, it is likely that a portion of the Cer can be "recycled" via hydrolysis. In addition, analogous prior studies showed that blockade of GlcCer synthase by 1-phenyl-2-decanoylamino-3-morpholino-1-propanol (PDMP) or 1-phenyl-2-palmitoylamino-3-morpholino-1-propanol (PPMP), specific inhibitors of GlcCer synthase, can lead to Cer accumulation in cells (47), whereas other GlcCer synthase inhibitors, *e.g. N*-butyldeoxynojirimycin, decrease GlcCer production without accumulation of Cer (48). These differences are thought to reflect 1-phenyl-2-decanoylamino-3-morpholino-1-propanol or 1-phenyl-2-palmitoylamino-3-morpholino-1-propanol, but not *N*-butyldeoxynojirimycin, inhibition of the conversion of Cer to 1-*O*-acylCer, resulting in Cer accumulation (49). Therefore, it remains possible that Cer-to-1-*O*-acylCer conversion might increase in cells when SM synthesis is blocked. In addition, the conversion of Cer to Cer 1-phosphate represents another pathway that could alter Cer metabolic fate. Although these metabolic pathways could contribute to the cellular Cer levels observed in keratinocytes treated with HPA-12, the increased Cer levels primarily reflect diminished SM generation through CERT inhibition.

Finally prior studies have also shown that CERT function can be modulated by oxysterols through the oxysterol-binding protein; *i.e.* 25-hydroxysterol binding to oxysterol-binding protein increases the interaction between CERT and the Golgi apparatus as well as between CERT and the ER (39, 50). Because alterations of hydroxysterol or hydroxysterol-binding protein levels have not been examined in cells under oxidative stress, it remains unknown the extent to which hydroxysterols are involved in the decreased CERT function observed in these cells following UVB irradiation.

In summary, decreases in SM generation in cultured human keratinocytes in response to oxidative stress are due, in part, to decreased CERT function, *i.e.* diminished Cer binding ability via the formation of a stable CERT homotrimer not previously appreciated. The formation of this CERT complex occurs not only in keratinocytes following UVB irradiation but also in extracutaneous cells, including HeLa and HEK293T. In addition, the oxidative stressors H_2O_2 and NO both also induce stable CERT homotrimer formation, revealing the more generalized formation of this stable transport protein complex. Thus, oxidative stress-induced stable CERT homotrimer formation represents a novel mechanism that can down-regulate both Cer transport and SM generation, which can produce potentially deleterious consequences for affected cells.

Acknowledgments—We gratefully acknowledge Dr. Peter M. Elias (Department of Dermatology, University of California, San Francisco and Department of Veterans Affairs Medical Center, San Francisco, CA) for numerous critical discussions. We thank Sally Pennypacker for expert technical support in cell culture and Sandra Chang and Sam Moradian for valuable technical assistance in morphological studies.

REFERENCES

1. Nishigori, C. (2006) *Photochem. Photobiol. Sci.* **5,** 208–214
2. Claerhout, S., Van Laethem, A., Agostinis, P., and Garmyn, M. (2006) *Photochem. Photobiol. Sci.* **5,** 199–207
3. Rabe, J. H., Mamelak, A. J., McElgunn, P. J., Morison, W. L., and Sauder, D. N. (2006) *J. Am. Acad. Dermatol.* **55,** 1–19
4. Larsson, P., Ollinger, K., and Rosdahl, I. (2006) *Br. J. Dermatol.* **155,** 292–300
5. Wang, Y., and Li, G. (2006) *J. Biol. Chem.* **281,** 11887–11893
6. Jinlian, L., Yingbin, Z., and Chunbo, W. (2007) *J. Biomed. Sci.* **14,** 303–312
7. Schwarz, A., Grabbe, S., Aragane, Y., Sandkuhl, K., Riemann, H., Luger, T. A., Kubin, M., Trinchieri, G., and Schwarz, T. (1996) *J. Investig. Dermatol.* **106,** 1187–1191
8. Ziegler, A., Jonason, A. S., Leffell, D. J., Simon, J. A., Sharma, H. W., Kimmelman, J., Remington, L., Jacks, T., and Brash, D. E. (1994) *Nature* **372,** 773–776
9. Zhang, W., Hanks, A. N., Boucher, K., Florell, S. R., Allen, S. M., Alexander, A., Brash, D. E., and Grossman, D. (2005) *Carcinogenesis* **26,** 249–257

10. Raj, D., Brash, D. E., and Grossman, D. (2006) *J. Investig. Dermatol.* **126,** 243–257
11. Mathias, S., Pena, L. A., and Kolesnick, R. N. (1998) *Biochem. J.* **335,** 465–480
12. Ruvolo, P. P. (2003) *Pharmacol. Res.* **47,** 383–392
13. Ohanian, J., and Ohanian, V. (2001) *CMLS Cell. Mol. Life Sci.* **58,** 2053–2068
14. Charruyer, A., Grazide, S., Bezombes, C., Muller, S., Laurent, G., and Jaffrezou, J. P. (2005) *J. Biol. Chem.* **280,** 19196–19204
15. Magnoni, C., Euclidi, E., Benassi, L., Bertazzoni, G., Cossarizza, A., Seidenari, S., and Giannetti, A. (2002) *Toxicol. In Vitro* **16,** 349–355
16. Uchida, Y., Nardo, A. D., Collins, V., Elias, P. M., and Holleran, W. M. (2003) *J. Investig. Dermatol.* **120,** 662–669
17. Itoh, M., Kitano, T., Watanabe, M., Kondo, T., Yabu, T., Taguchi, Y., Iwai, K., Tashima, M., Uchiyama, T., and Okazaki, T. (2003) *Clin. Cancer Res.* **9,** 415–423
18. Liu, Y. Y., Han, T. Y., Giuliano, A. E., and Cabot, M. C. (1999) *J. Biol. Chem.* **274,** 1140–1146
19. Uchida, Y., Itoh, M., Taguchi, Y., Yamaoka, S., Umehara, H., Ichikawa, S., Hirabayashi, Y., Holleran, W. M., and Okazaki, T. (2004) *Cancer Res.* **64,** 6271–6279
20. Grazide, S., Terrisse, A. D., Lerouge, S., Laurent, G., and Jaffrezou, J. P. (2004) *J. Biol. Chem.* **279,** 18256–18261
21. Bonhoure, E., Pchejetski, D., Aouali, N., Morjani, H., Levade, T., Kohama, T., and Cuvillier, O. (2006) *Leukemia* **20,** 95–102
22. Uchida, Y., Murata, S., Schmuth, M., Behne, M. J., Lee, J. D., Ichikawa, S., Elias, P. M., Hirabayashi, Y., and Holleran, W. M. (2002) *J. Lipid Res.* **43,** 1293–1302
23. Fukasawa, M., Nishijima, M., and Hanada, K. (1999) *J. Cell Biol.* **144,** 673–685
24. Funakoshi, T., Yasuda, S., Fukasawa, M., Nishijima, M., and Hanada, K. (2000) *J. Biol. Chem.* **275,** 29938–29945
25. Hanada, K., Kumagai, K., Yasuda, S., Miura, Y., Kawano, M., Fukasawa, M., and Nishijima, M. (2003) *Nature* **426,** 803–809
26. Alpy, F., and Tomasetto, C. (2005) *J. Cell Sci.* **118,** 2791–2801
27. Kudo, N., Kumagai, K., Tomishige, N., Yamaji, T., Wakatsuki, S., Nishijima, M., Hanada, K., and Kato, R. (2008) *Proc. Natl. Acad. Sci. U. S. A.* **105,** 488–493
28. Kawano, M., Kumagai, K., Nishijima, M., and Hanada, K. (2006) *J. Biol. Chem.* **281,** 30279–30288
29. Kumagai, K., Kawano, M., Shinkai-Ouchi, F., Nishijima, M., and Hanada, K. (2007) *J. Biol. Chem.* **282,** 17758–17766
30. Yasuda, S., Kitagawa, H., Ueno, M., Ishitani, H., Fukasawa, M., Nishijima, M., Kobayashi, S., and Hanada, K. (2001) *J. Biol. Chem.* **276,** 43994–44002
31. Pittelkow, M. R., and Scott, R. E. (1986) *Mayo Clin. Proc.* **61,** 771–777
32. Haratake, A., Uchida, Y., Schmuth, M., Tanno, O., Yasuda, R., Epstein, J. H., Elias, P. M., and Holleran, W. M. (1997) *J. Investig. Dermatol.* **108,** 769–775
33. Pagano, R. E., Martin, O. C., Kang, H. C., and Haugland, R. P. (1991) *J. Cell Biol.* **113,** 1267–1279
34. Koval, M., and Pagano, R. E. (1991) *Biochim. Biophys. Acta* **1082,** 113–125
35. Malakhova, M. L., Malinina, L., Pike, H. M., Kanack, A. T., Patel, D. J., and Brown, R. E. (2005) *J. Biol. Chem.* **280,** 26312–26320
36. Bligh, E. G., and Dyer, W. J. (1959) *Can. J. Biochem. Physiol.* **37,** 911–917
37. Holleran, W. M., Uchida, Y., Halkier-Sorensen, L., Haratake, A., Hara, M., Epstein, J. H., and Elias, P. M. (1997) *Photodermatol. Photoimmunol. Photomed.* **13,** 117–128
38. Oberhammer, F. A., Pavelka, M., Sharma, S., Tiefenbacher, R., Purchio, A. F., Bursch, W., and Schulte-Hermann, R. (1992) *Proc. Natl. Acad. Sci. U. S. A.* **89,** 5408–5412
39. Perry, R. J., and Ridgway, N. D. (2006) *Mol. Biol. Cell* **17,** 2604–2616
40. Huwiler, A., Pfeilschifter, J., and van den Bosch, H. (1999) *J. Biol. Chem.* **274,** 7190–7195
41. Martin, D., Salinas, M., Fujita, N., Tsuruo, T., and Cuadrado, A. (2002) *J. Biol. Chem.* **277,** 42943–42952
42. Chujor, C. S., Feingold, K. R., Elias, P. M., and Holleran, W. M. (1998) *J. Lipid Res.* **39,** 277–285
43. Halter, D., Neumann, S., van Dijk, S. M., Wolthoorn, J., de Maziere, A. M., Vieira, O. V., Mattjus, P., Klumperman, J., van Meer, G., and Sprong, H. (2007) *J. Cell Biol.* **179,** 101–115
44. Lupas, A., Van Dyke, M., and Stock, J. (1991) *Science* **252,** 1162–1164
45. Fugmann, T., Hausser, A., Schoffler, P., Schmid, S., Pfizenmaier, K., and Olayioye, M. A. (2007) *J. Cell Biol.* **178,** 15–22
46. Houben, E., Holleran, W. M., Yaginuma, T., Mao, C., Obeid, L. M., Rogiers, V., Takagi, Y., Elias, P. M., and Uchida, Y. (2006) *J. Lipid Res.* **47,** 1063–1070
47. Abe, A., Radin, N. S., Shayman, J. A., Wotring, L. L., Zipkin, R. E., Sivakumar, R., Ruggieri, J. M., Carson, K. G., and Ganem, B. (1995) *J. Lipid Res.* **36,** 611–621
48. Bieberich, E., Freischutz, B., Suzuki, M., and Yu, R. K. (1999) *J. Neurochem.* **72,** 1040–1049
49. Lee, L., Abe, A., and Shayman, J. A. (1999) *J. Biol. Chem.* **274,** 14662–14669
50. Wyles, J. P., McMaster, C. R., and Ridgway, N. D. (2002) *J. Biol. Chem.* **277,** 29908–29918